Physica C 193 (1992) 178–188
North-Holland

PHYSICA C

High pressure synthesis and structural study of R_2CuO_4 compounds with R = Y, Tb, Dy, Ho, Er, Tm

P. Bordet [a], J.J. Capponi [a], C. Chaillout [a], D. Chateigner [a], J. Chenavas [a], Th. Fournier [a,c], J.L. Hodeau [a], M. Marezio [a,b], M. Perroux [a], G. Thomas [d] and A. Varela [a]

[a] *Laboratoire de Cristallographie CNRS-UJF, BP 166X, 30842 Grenoble Cedex, France*
[b] *AT&T Bell Laboratories, Murray Hill, NJ 07974, USA*
[c] *CRTBT, CNRS, BP 166X, 30842 Grenoble Cedex, France*
[d] *Department of Materials Science and Mineral Engineering, National Center for Electron Microscopy, University of California, Berkeley, CA 94720, USA*

Received 13 January 1992

The title compounds have been prepared by high pressure/high temperature reaction. Thermogravimetric measurements indicate that they decompose above ≈350°C in He flow. Electron microscopy and X-ray powder and single crystal diffraction data are presented. They all reveal the presence of three types of superstructure, corresponding to different unit cells, which can be observed in different grains of the same sample. The results of an average structure refinement carried out with the unit cell, and symmetry of the T′ phase are presented for the Tm_2CuO_4 compound. These results are compared with those obtained for Gd_2CuO_4.

1. Introduction

The compounds corresponding to the R_2CuO_4 chemical formula, where R denotes a rare-earth element, are known to exist for R ranging from La to Gd and exhibit extremely interesting physical properties. La_2CuO_4 has the K_2NiF_4-type T structure and has been extensively studied as a p-type high-temperature superconductor when doped with excess oxygen with a large divalent cation. The R_2CuO_4 compounds with R = Pr, Nd, Sm and Eu become n-type high temperature superconductors when the R cations are partially substituted by tetravalent cations. They have the Nd_2CuO_4 T′ structure containing square-coordinated Cu cations and eight-coordinated R cations. Although it has the same structure, Gd_2CuO_4 does not become superconducting through doping.

For heavier rare-earth cations (R = Tb to Lu), the R_2CuO_4 compounds cannot be prepared at ambient pressure and compounds with the $R_2Cu_2O_5$ formula are usually formed. Recently, it has been shown that the R_2CuO_4 compounds with R = Tb to Tm can be prepared under high pressure and that they present the T′ structure [1]. We present here results on the synthesis conditions, stability and crystal structure of these new compounds.

2. Sample preparation

Powder samples of R_2CuO_4 (R = Y, Tb, Dy, Ho, Er, Tm) were obtained by high-pressure and high-temperature reactions using a high-pressure belt-type apparatus. The maximum pressure and temperature were 9 GPa and 1500°C, respectively. Stoichiometric mixtures of copper and rare-earth oxides were thoroughly ground and sealed in platinum capsules. Various experimental conditions were tried in order to determine the range of stability of the R_2CuO_4 phase for each R element (R = Y, Tb, Dy, Ho, Er, Tm, Yb and Lu). For every experiment, the pressure was first increased to the nominal value at a rate of ≈0.2 GPa/mn, then the temperature was raised to the desired value at ≈100°C/mn. The pressure and the temperature were kept constant for one hour, after which the furnace power supply was shut off and the pressure was decreased to normal within ≈one hour.

The samples were checked by energy-dispersive microanalysis, using a Kevex Delta class analyzer installed on a JSM 840-A scanning electron microscope, and by X-ray powder diffraction, using a Guinier camera and Fe Kα radiation. The films were digitalized with a LS20 line scanner and the Bragg angles were obtained with the reflexion positions of a Si internal standard.

The R_2CuO_4 phase was obtained for R = Y, Tb, Dy, Ho, Er and Tm. For Y, it was observed at pressures and temperatures above 5 GPa and 900°C, while for Tb, Dy, Ho and Er the minimum values at which the phase was obtained were ≈8 GPa and 1000°C. The Tm_2CuO_4 phase was obtained at 9 GPa and 1200°C. For smaller rare-earths such as Yb and Lu, the R_2CuO_4 phase could not be obtained. For R = Y, Tb, Dy, Ho, Er and Tm, the inner part of the pellets obtained corresponded to the R_2CuO_4 composition as revealed by microanalysis, with very small inclusions of copper oxide. The outer part consisted of a thin layer of a parasitic phase. Microanalysis and X-ray diffraction showed that this phase corresponded to the high pressure phase B-R_2O_3 [2]. Since this parasitic phase was only present at the surface of the pellets, it could be easily removed by scraping the surface.

During one run for the Tm_2CuO_4 phase the pellet contained single crystals about 0.1 mm in size. Similar single crystals of the Y_2CuO_4 phase were synthesized by slow-cooling (2°C/mn) a stoichiometric mixture of Y_2O_3 and CuO under high pressure. This technique should allow us to grow single crystals of the R_2CuO_4 phase for the other rare-earth cations.

3. Thermogravimetry

The stability of these high-pressure phases with respect to temperature was checked by thermogravimetric experiments. A Perkin-Elmer TGA 7 thermogravimetric analyzer was used. The samples placed in a Pt container were heated to 800°C at 2°C/mn in a He flow. The reducing atmosphere was chosen because such an atmosphere is needed to obtain superconducting samples of the Ce doped Nd_2CuO_4 phase. A typical thermogravimetric curve is reported in fig. 1 for the Y_2CuO_4 compound. The

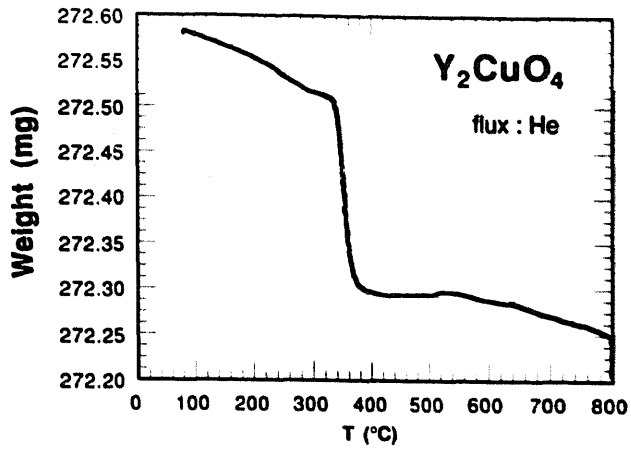

Fig. 1. TGA curve obtained for Y_2CuO_4 in He atmosphere.

sample weight remains approximately constant up to ≈300°C, where an abrupt weight loss is observed. A second and more pronounced weight loss is visible above ≈800°C. For all the R_2CuO_4 compounds, the first weight loss occurred between 300 and 350°C. Guinier films taken with samples annealed at temperatures between the two weight losses indicated that the R_2CuO_4 phase decomposed. This result shows that it is not possible to keep the R_2CuO_4 phase after high-temperature annealing in a reducing atmosphere. This could be the reason why these compounds do not become n-type superconductors.

4. Electron microscopy

Two different instruments were used for the electron microscopy/diffraction studies: a Philips EM400 T (120 kV) at the C.N.R.S. Grenoble, and a Jeol 200CX (200 kV) at the L.B. L., Berkeley. Each microscope was equipped with a double tilting goniometer stage in order to reach as many planes as possible in reciprocal space with the same sample.

For the samples of Y_2CuO_4 and Tm_2CuO_4 obtained under high pressure, the strongest reflexions corresponded to the Nd_2CuO_4-type cell $a_p \times a_p \times c$ ($c \approx 11.7$ Å); however, three different supercells were found to exist for both compounds, depending on the grain observed:

- (α) superstructure corresponding to a $2a_p\sqrt{2} \times a_p\sqrt{2} \times c$ cell

- (β) superstructure corresponding to a $2a_p\sqrt{2}\times 2a_p\sqrt{2}\times 2c$ cell
- (γ) superstructure corresponding to a $a_p\sqrt{2}\times a_p\sqrt{2}\times c$ cell.

The (α) superstructure was the most commonly present in Y_2CuO_4. It is characterised by strong (1/2 1/2 0) and (1/4−1/4 0) reflexions and weak (1/2−1/2 0) ones (figs. 2(a,b)). The absence of (1/2 0 0), (1/4 0 0), (0 1/2 0), (0 1/4 0), etc... reflexions when the multiple scattering is not present indicates that this (α) superstructure can as a first approximation be characterized by two components that are weakly linked, namely a (1/2 1/2 0) superstructure along $(a+b)$ and a (1/4−1/4 0) modulation along $(a-b)$. Along this direction, the first order reflexions (1/4−1/4 0) are much stronger than those of the second order (1/2−1/2 0), and diffuse lines parallel to this direction are observed. This indicates that this modulation is nearly sinusoidal and presents stacking faults.

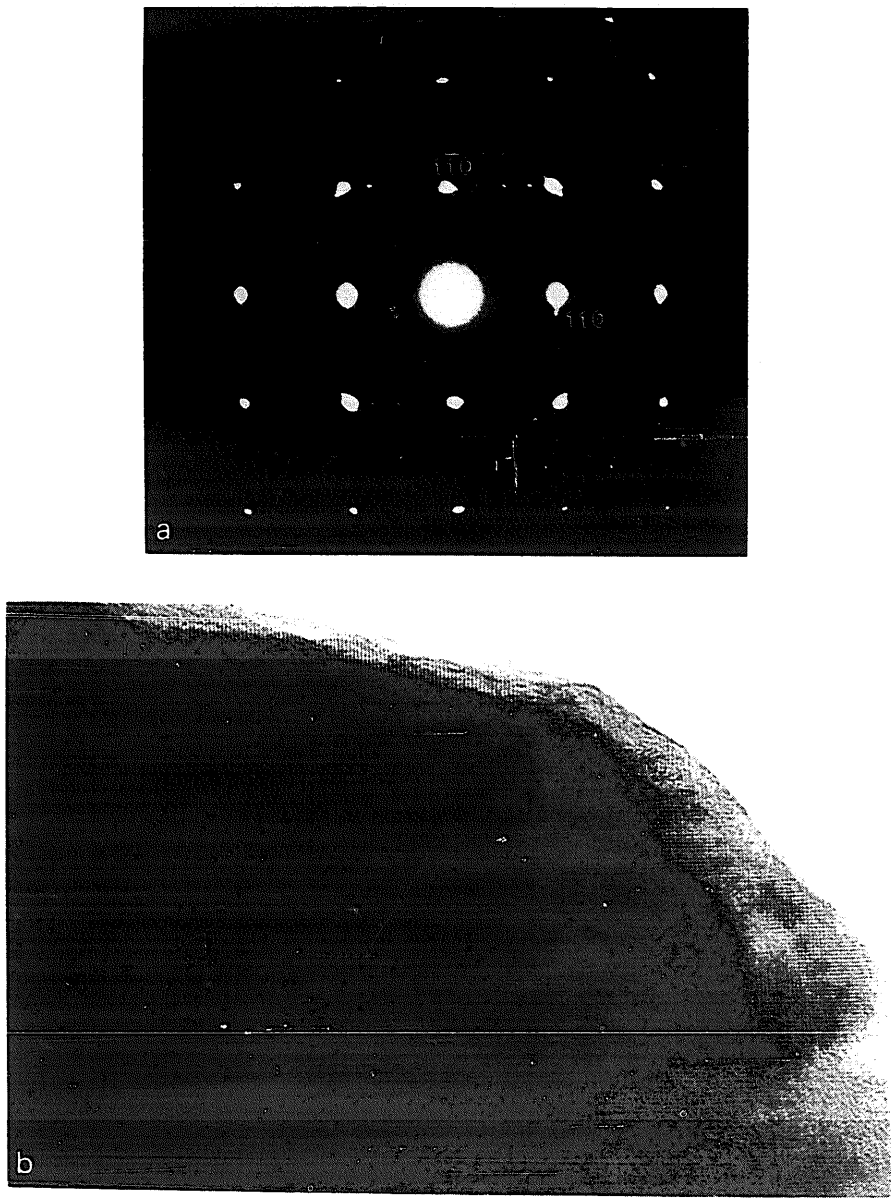

Fig. 2. (a): [001] zone axis electron diffraction pattern from Y_2CuO_4 sample showing reflexions from the (α) superstructure. (b): corresponding high-resolution image.

The (β) superstructure could be observed clearly in Tm_2CuO_4 samples (fig. 3(a)) and was also present, but weakly, in Y_2CuO_4 samples. This superstructure is analogous to that reported by Chen et al. [3] for Ce-doped Nd_2CuO_4 compounds; however, the superstructure reflexion intensities seem to be weaker in our case. Chen et al. reported that the superstructure spots were due to two domains, and only a one-dimensional superstructure in the plane perpendicular to the [001] direction was found by inspecting a single domain grain. The same behaviour is true for our samples. It is due to the extinction condition, corresponding to the A-centered space-group, observed in grains oriented perpendicularly to each other. Instead, in Tm_2CuO_4, we found a two-dimensional superstructure in a single domain. A high resolution image of this sample reveals the small domain size. Figure 3(b) is a low magnification HREM image corresponding to the ED pattern of fig. 3(a). In part A of one grain the superstructure is along one direction, and dislocations are visible. But in another grain the two-dimensional superstructure has been found in part B (fig. 3(c)). The overlapping of two domains perpendicular to each other, each presenting the one-dimensional superstructure, could explain this observation. As can be seen in fig. 3(c), the contrast of the (β) superstructure is wavy, as in a sinusoidal modulation, and its periodicity is four times the (1 1 0) d-spacing.

The third superstructure (γ) is very weak and diffuse in both Y_2CuO_4 and Tm_2CuO_4 d compounds (fig. 4(a)) and seems to exist only in very small grains. The superstructure intensities are much weaker than those of the subcell. Figure 4(b) is the HREM image corresponding to the figure 4(a) pattern: in parts A and B the ordering directions are perpendicular to each other, as two domains. In part C two kinds of superstructures can be seen within one domain. The contrast change through the superstructure is sharp, which is contrary to that observed for (β) superstructure.

Besides the difference in vector length among these different superstructures, their cause may also be different. The intensity of the (α) superstructure reflexions is nearly as strong as that of the subcell. These (α) and (β) superstructures are probably produced by a displacive cation modulation rather than only by oxygen ordering. On the other hand, in the (γ) superstructure the intensity of the superstructure reflexions is much lower than that of the subcell reflexions and this superstructure could be related to an oxygen/vacancy ordering phenomenon or to oxygen displacements.

5. Comparison with Gd_2CuO_4

In order to check whether or not similar superstructures could be observed in ambient pressure-prepared R_2CuO_4 compounds, we performed an electron diffraction study of a Gd_2CuO_4 sample. This compound was chosen because it is the last member which can be prepared at ambient pressure and it does not become superconducting when doped with Ce. Moreover, Galez et al. [4] recently reported a single-crystal X-ray diffraction study of this compound showing the existence of a structural distortion, but no superstructure has been reported up to now for Gd_2CuO_4.

The sample used for the electron diffraction study was obtained by crushing a flux-grown single crystal. The same three types of superstructures as described above for Y_2CuO_4 and Tm_2CuO_4 were indeed observed for Gd_2CuO_4. In this case, the (β) superstructure was the most commonly found and the superstructure reflexions were rather strong. Figure 5 shows that the modulation in the [001] plane occurs only along the [110] (or [1-10]) direction. However, depending on the crystal area observed, the superstructure reflexions can be seen along the perpendicular direction. This indicates the presence of domains for the high-pressure-grown samples. It is also similar to the observations of Chen et al. for the Ce-doped Nd_2CuO_4 compound [3]. As reported by the latter, the $[-1\,1\,1]$, $[1-1\,1]$ and $[1\,1\,1]$ zone axes are not equivalent (figs. 6(a–c)), because the superstructure reflexions are present in rows parallel to only one [112]-type direction. The extinction conditions of the different patterns indicate that the lattice is A-centered.

Some crystals presented the (γ) superstructure (figs. 7(a) and 7(b) as well. In this case, the spots at (1/2 1/2 0) and equivalent positions are very sharp and strong. We noticed that when the sample was beam-heated, additional weak superstructure reflexions appeared at (1/4 1/4 0), (3/4 3/4 0) and

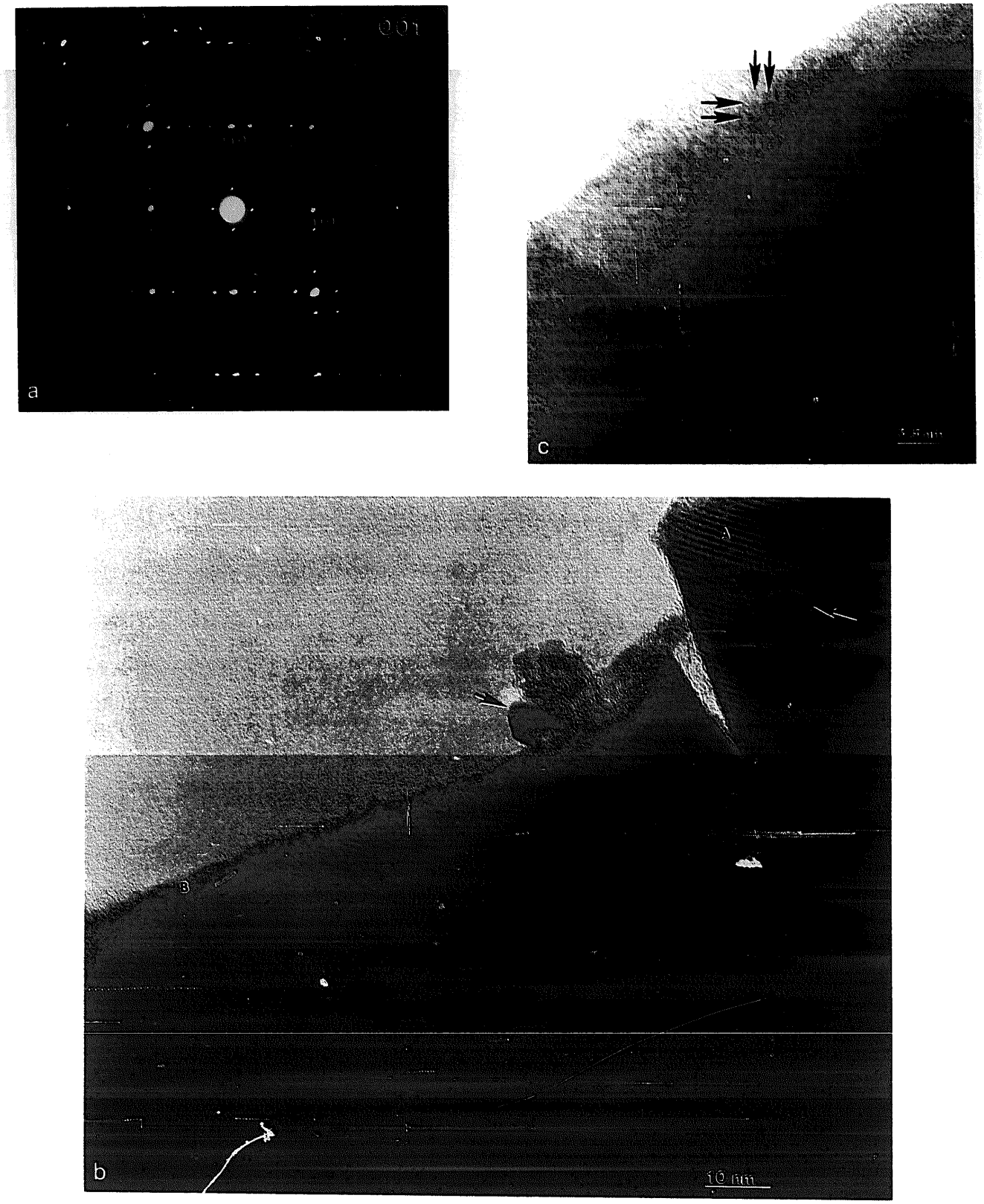

Fig. 3. (a): [001] zone axis electron diffraction pattern from Tm_2CuO_4 sample showing reflexions from the (β) superstructure. (b): corresponding low-magnification, high-resolution image. (c): higher magnification from part B of (b).

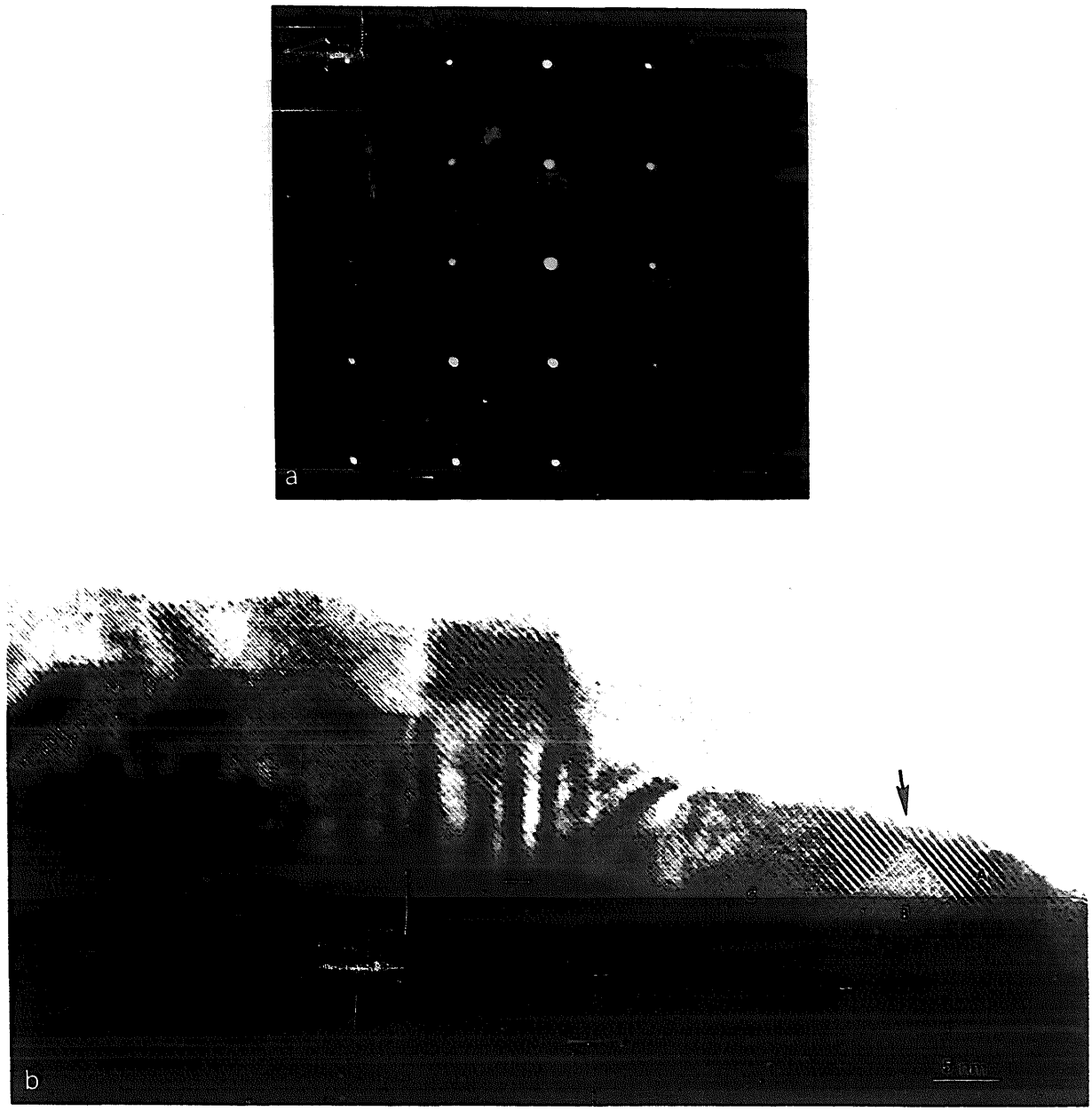

Fig. 4. (a): [001] zone axis electron diffraction pattern from Tm_2CuO_4 sample showing reflexions from the (γ) superstructure. (b): corresponding high-resolution image.

equivalent positions, leading to the (α) superstructure. These weak reflexions disappeared when the sample irradiation decreased.

It can be concluded that the same types of ordering exist in Gd_2CuO_4 and in the high-pressure synthesized R_2CuO_4 compounds. All these samples are far from homogeneous and the relative proportions of each type of superstructure are strongly sample-dependent. This seems to indicate that the superstructures are related to deformations of the lattice taking place to accommodate the small rare-earth cations and thus are very sensitive to the sizes of these cations. The (γ)→(α) transformation observed for Gd_2CuO_4 could also exist in the high-pressure synthesized R_2CuO_4 compounds at somewhat lower temperatures. This could explain why the (α) su-

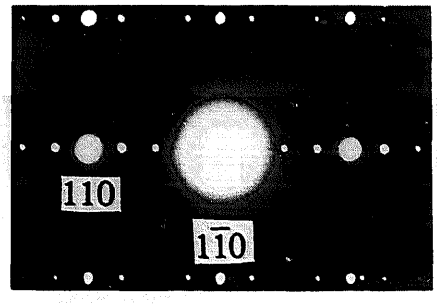

Fig. 5. [001] zone axis electron diffraction pattern for Gd_2CuO_4.

perstructure is very often observed for the latter. The (γ) superstructure is very weak and of short range. However, since several superstructures are present in a given sample, the complete determination by diffraction techniques of the corresponding structural distortions will be extremely difficult.

6. X-ray powder diffraction

As a first approximation, the Guinier films of the R_2CuO_4 compounds synthesized under high pressure can all be indexed with the Nd_2CuO_4-type unit cell and the I4/mmm space group. Figures 8(a) and 8(b) represent the variation of the cell parameters and of the c/a ratio versus the ionic radii of the rare-earth cations taken from reference [5]. These results are in qualitative agreement with those reported by ref. [1]. The values for the R_2CuO_4 compounds with R=Pr–Gd obtained by solid state reaction at ambient pressure are included for comparison. Contrary to what one would expect, the cell parameters do not vary linearly as a function of the ionic radii and the deviation from linearity is even more pronounced for the c/a ratio. Three different behaviours can be distinguished in the c/a versus r curve. One corresponds to rare-earth cations smaller than Tb where the c/a ratio varies linearly. A second corresponds to the rare-earth cations larger than Eu where the c/a ratio also varies linearly but with a slope different from that corresponding to the small rare-earth cations. The third behaviour corresponds to Eu, Gd and Tb for which the c/a ratios are intermediate between the previous two. This can be related to the existence of structural distortions, as revealed by electron microscopy for the R_2CuO_4 compounds with small rare-earth cations.

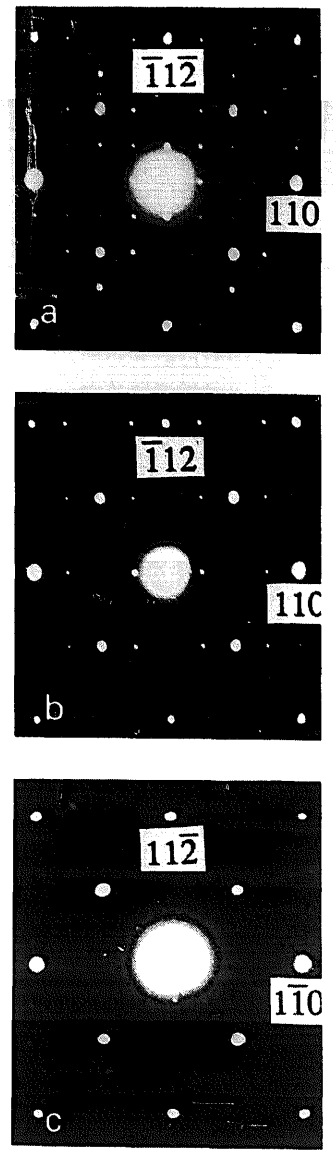

Fig. 6. (a): [−111] zone axis electron diffraction pattern for Gd_2CuO_4. (b): [1−11] zone axis electron diffraction pattern. (c): [111] zone axis electron diffraction pattern.

A closer analysis of the Guinier films revealed the presence of many extra, weak reflexions. These extra reflexions could be indexed in one of the superstructure cells determined by electron microscopy and single-crystal X-ray diffraction (see below). The largest superstructure unit cell is orthorhombic with parameters $a_s \approx 2a_p\sqrt{2}$, $b_s \approx 2a_p\sqrt{2}$ and $c_s \approx 2c$. Owing to the very large size of this unit cell (≈ 2500 Å^3) and to the pseudo-symmetry, the indexing of the Guinier films is not unambiguous. Nevertheless, a

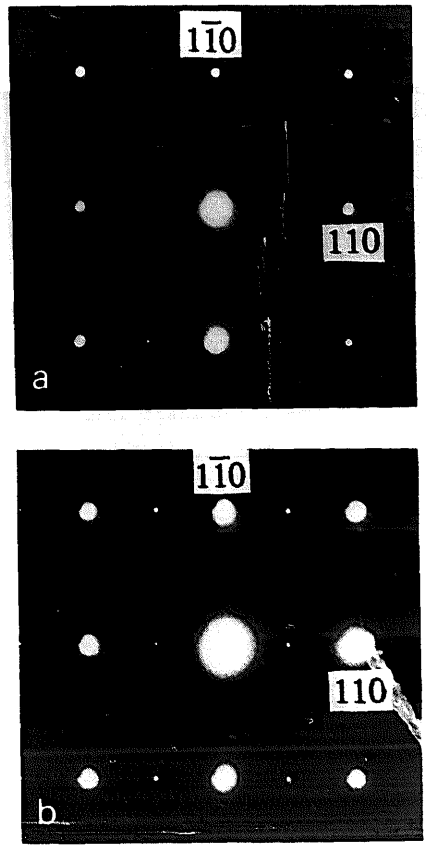

Fig. 7. [001] zone axis electron diffraction pattern for Gd_2CuO_4. (a): Sharp spots are present at (1/2 1/2 0) and equivalent positions. (b): same pattern after beam-heating.

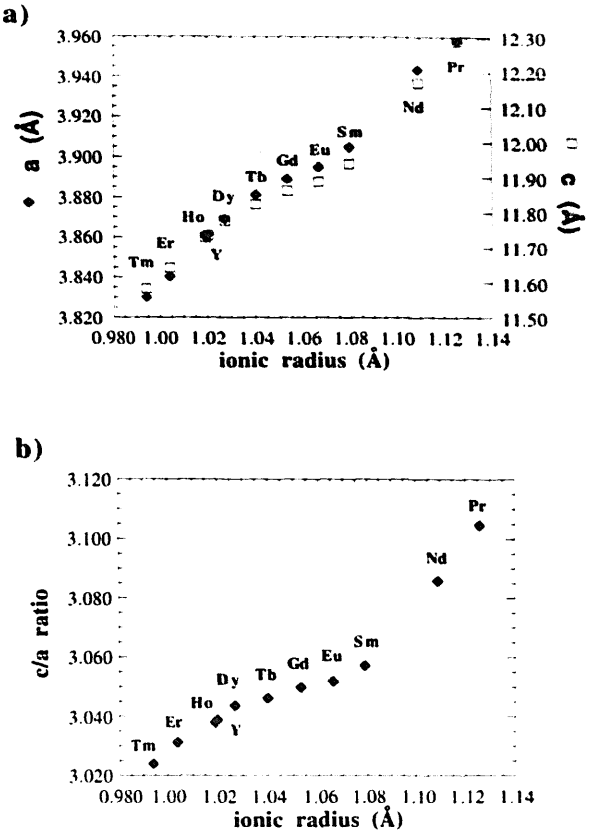

Fig. 8. Variation of the a- and c-cell parameters (a) and c/a ratio (b) for the R_2CuO_4 compounds vs. the ionic radii of the rare-earth cations.

satisfactory indexing of the Tm_2CuO_4 Guinier film could be obtained by comparison with the single-crystal data collected from the above superstructure cell. The corresponding Guinier film is shown in fig. 9 and its indexing is given in table 1. The reflexions reported in table 1 are indexed on the $2a_p\sqrt{2}\times a_p\sqrt{2}\times c$ unit cell of the (α) superstructure described above. Actually, there are about 10 more very weak, extra reflexions which can be indexed on the $2a_p\sqrt{2}\times 2a_p\sqrt{2}\times 2c$ cell, but most of them do not respect the A-centering condition found by electron diffraction and none could be observed by single-crystal X-ray diffraction. They could be attributed to small amounts of parasitic phases. Therefore, for this sample, the (α)-type superstructure seems to be predominant over the (β)-type one. The cell parameters obtained are $a_s=10.8388(9)$ Å, $b_s=5.4341(4)$ Å and $c_s=11.5984(7)$ Å.

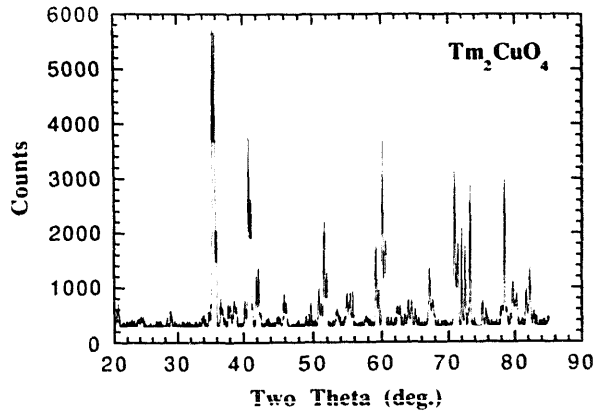

Fig. 9. Guinier film obtained for the Tm_2CuO_4 compound (Fe Kα radiation). The lines from the Si standard are marked with a dot.

7. Single-crystal X-ray diffraction

We chose to study by X-ray diffraction a single

Table 1
Indexation of the Guinier film obtained for Tm_2CuO_4. The reflexions are indexed on the $2a_p\sqrt{2}\times a_p\sqrt{2}\times c$ unit cell corresponding to the (α) superstructure

h k l	Theta obs.	Theta calc.	Difference	I (%)
1 1 2	15.068	15.077	−0.009	1.31
2 1 1	15.413	15.42	−0.007	24.20
3 0 2	18.409	18.414	−0.005	2.18
1 1 3	18.673	18.676	−0.003	8.67
3 1 1	19.426	19.427	−0.001	5.62
0 0 4	19.518	19.515	0.003	4.41
2 1 3	20.837	20.834	0.003	100.00
0 2 0	20.885	20.886	−0.001	23.57
4 0 0	20.945	20.945	0	17.45
1 2 1	22.148	22.142	0.006	3.05
0 2 2	23.201	23.185	0.016	1.87
4 1 1	24.087	24.085	0.002	2.09
0 2 4	29.257	29.246	0.011	29.91
1 2 4	29.785	29.78	0.005	3.43
0 0 6	30.077	30.072	0.005	16.49
4 2 0	30.323	30.322	0.001	75.80
5 1 2	30.609	30.614	−0.005	3.28
4 1 4	31.382	31.381	0.001	1.93
3 1 5	31.826	31.822	0.004	2.87
2 0 6	32.148	32.142	0.006	1.06
6 0 0	32.415	32.426	−0.011	1.75
5 1 3	32.855	32.848	0.007	3.43
5 0 4	33.907	33.912	−0.005	3.66
1 3 2	34.569	34.564	0.005	7.37
4 1 5	35.317	35.301	0.016	1.71
5 2 2	36.553	36.551	0.002	1.78
1 3 3	36.663	36.674	−0.011	1.50
4 2 4	37.244	37.256	−0.012	2.00
4 0 6	37.98	37.991	−0.011	33.19
2 3 3	38.097	38.097	0	42.40
1 1 7	38.138	38.147	−0.009	63.53
1 2 6	38.408	38.421	−0.013	11.42
6 0 4	39.191	39.18	0.011	1.59
1 3 4	39.548	39.556	−0.008	8.87
7 1 1	40.986	40.982	0.004	3.37
3 1 7	41.864	41.867	−0.003	2.43
0 0 8	41.922	41.922	0	1.87

crystal of the Tm_2CuO_4 compound, which should present a large distortion of the basic R_2CuO_4 structure because of the relatively small Tm ionic radius. An irregularly-shaped, single crystal was first examined by X-ray diffraction with a precession camera. It was then mounted on a Philips PW 1100 diffractometer equipped with graphite monochromatized Ag Kα radiation. The lattice parameters of the (a_p, a_p, c) unit cell were refined from the position of 18 reflexions with Bragg angles ranging from 8° to 12°. Scans of reflexions that could be indexed on the (α), (β) and (γ) superstructure unit cells were performed. It became evident that the largest unit cell (that is the ($2a_p\sqrt{2}$, $2a_p\sqrt{2}$, $2c$) unit cell of the (β) superstructure) had to be taken into account in order to index all reflexions. The A-centering extinction condition observed by electron diffraction was also verified for this single crystal.

All reflexions up to $\theta=20°$ were collected. Those which did not obey the A-centering condition were

omitted. The scan width was 1.4°, with 0.02° s^{-1} scan speed. Between one and three consecutive scans were carried out according to the intensity. Detector slits of 1×1 mm^2 were used. A total of 3838 reflexions were measured and corrected for Lorentz-polarization effects.

In order to determine the percentage of the different superstructures, statistical tests on the intensities after averaging them in the Ammm space group were carried out. Of the 990 independent reflexions, 103 belonged to the (a_p, a_p, c) I-centered unit cell of the T′ structure, of which 101 had $I > \sigma$ and 80 $I > 10\sigma$; 86 belonged to the same cell but did not obey the I-centering condition, of which 71 had $I > \sigma$ and 24 $I > 10\sigma$; 125 reflexions (with h and l even) belonged to the ($a_p\sqrt{2}$, $a_p\sqrt{2}$, c) unit cell of the (γ) superstructure, of which 103 had $I > \sigma$ and 36 $I > 10\sigma$; 333 reflexions (with h odd and l even) belonged to the ($2a_p\sqrt{2}$, $a_p\sqrt{2}$, c) unit cell of the (α) superstructure, of which 288 had $I > \sigma$ and 187 $I > 10\sigma$; and finally, 343 reflexions (with k and l odd) belonged to the A-centered ($2a_p\sqrt{2}$, $2a_p\sqrt{2}$, $2c$) unit cell of the (β) superstructure, of which 25 had $I > \sigma$ and none had $I > 10\sigma$.

The intensity of the superstructure reflexions is far from being negligible and the structural distortions producing these reflexions must be large, with an appreciable contribution coming from the cations. Moreover, it should be pointed out that the reflexions, which are indexable only on the unit cell of the β superstructure, are very weak or unobserved. A typical scan of one of the strongest reflexions of this type (1 −3 3) is shown in fig. 10 and compared with the (1 2 4) reflexion indexable in the (α) superstructure unit cell. Consequently, the influence of the (β) superstructure could probably be neglected in the first attempt to solve this complex structural problem. Since the strongest contribution is coming from the (α) superstructure, the corresponding unit cell, ($2a_p\sqrt{2}$, $a_p\sqrt{2}$, c) could be used. However, attempts to refine the structure with this unit cell and various orthorhombic space groups have failed so far to give reasonable results.

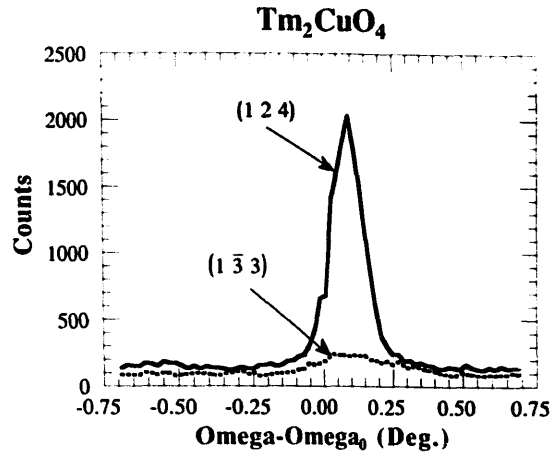

Fig. 10. ω-scans of the (1 −3 3) and (1 2 4) reflexions (indexed in the (α) superstructure unit cell) for a Tm_2CuO_4 single crystal.

The preliminary results of a least square refinement of the average structure with the I-centered (a_p, a_p, c) unit cell and I4/mmm space group of the T′ phase are presented in table 2. The corresponding interatomic distances are also given. Data processing and refinements were carried out by the SDP program package [6]. After index transformation and averaging in the 4/mmm point group, 65 indepen-

Table 2
Positions, thermal factors (Å^2) and interatomic distances (Å) for Tm_2CuO_4 as determined by average structure refinement with the T′ unit cell and space group

atom	pos.	x	y	z	U_{11}	U_{22}	U_{33}
Tm	4e	0	0	0.34579(9)	0.0255(7)	0.0255	0.0364(5)
Cu	2a	0	0	0	0.014(2)	0.014	0.006(1)
O(1)	8j	0.091(7)	1/2	0	0.007(25)	0.007(12)	0.11(1)
O(2)	4d	0	1/2	1/4	0.022(9)	0.022	0.078(8)

Cu–O(1) (×4)	1.950(5)	Tm–O(1) (×2)	2.89(2)
Tm–O(1) (×2)	2.38(2)	Tm–O(2)(×4)	2.216(1)
average Tm–O distance:	2.43(32)		

dent reflexions with $I > \sigma$ were retained. The absorption correction was made by using the DIFABS program of Walker and Stuart [7]. The starting atomic positions were Cu in 2a (0 0 0), Tm in 4e (0 0 z=.33), O(1) in 4c (0 1/2 0) and O(2) in 4d (0 1/2 1/4). Statistical weights ($1/\sigma^2$) were used. The reliability factors $R=6.1\%$ and $wR=3.5\%$ were obtained by allowing the scale factor, the z-coordinate of Tm and the anisotropic thermal parameters for all atoms to vary. A very large value (0.19 Å^2) was obtained for the U_{11} parameter of the O(1) atom. Thus, it was placed in the disordered 8j (x 1/2 0) position, and x was refined together with the other parameters. This refinement yielded $R=5.8\%$ and $wR=3.3\%$ reliability factors. As these refinements cannot give anything more than an average structure we decided not to go any further.

This average structure is very similar to that reported by Galez et al. [3] for Gd_2CuO_4, for which a displacement of the O(1) atom along the a-axis was also found. However, the displacement found for Tm_2CuO_4 ($x=0.091$) is approximately twice as large as that found for Gd_2CuO_4 ($x=0.046$). This larger O(1) displacement observed for Tm_2CuO_4 is probably the result of a larger structural distortion due to the smaller size of Tm^{3+} compared to that of Gd^{3+}.

Additional studies are underway in order to go beyond this average description of the structure of Tm_2CuO_4 and of the R_2CuO_4 compounds with R=Gd, Tb, Dy, Ho and Er. However, the electron microscopy results indicate that several types of superstructure may coexist in different areas of the same sample, which complicates the complete solution of the structure.

References

[1] H. Okada, M. Takano and Y. Takeda, Physica C 166 (1990) 111.
[2] H.R. Hoekstra, Inorg. Chem. 5-5 (1966) 754.
[3] C.H. Chen, D.J. Werder, A.C.W.P. James, D.W. Murphy, S. Zahurak, R.M. Fleming, B. Batlogg and L.F. Schneemeyer, Physica C 160 (1989) 375.
[4] Ph. Galez and G. Colin, J. Phys. (Paris) 51 (1990) 579.
[5] R.D. Shannon, Acta Crystallogr. A32 (1976) 751.
[6] Structure Determination Package, B.A. Frenz and Associates, Inc., (1985).
[7] N. Walker and D. Stuart, Acta Crystallogr. A39 (1983) 158.